GLOBAL IRRADIANCE: TYPICAL YEAR AND YEAR TO YEAR ANNUAL VARIABILITY

Pierre Ineichen

University of Geneva, Institute for Environmental Science, Geneva (Switzerland)

1. Introduction

Models converting satellite images into the different radiation components become increasingly performing and give often better estimation of the solar irradiation availability than ground measurements if the station is not situated in the near vicinity of the application.

Two different kinds of models are used to circumvent the lack of ground measurements: «average» models based on 10 to 20 years of ground measurements and interpolation between stations, and satellite based models that give «real» time series for specific years.

The present study analyzes the interannual variability (variation from one year to the other) of the solar irradiation and compares it to the corresponding annual irradiation obtained from different evaluation models.

2. Ground measurements

Data from 21 European and African, and 6 American ground stations were collected to conduct the study. The geographic locations of the stations cover latitudes from 8°N to 58°N, altitudes from sea level to 3000 m and a great variety of climates. For stations part of the SurfRad, BSRN (http://www.gewex.org/bsrn.html) and CIE (CIE 1994) networks, high precision instruments (WMO 2008) such as Kipp and Zonen CM10 and Eppley PSP pyranometers, are used to acquire the data. For the other stations, it was not possible to determine the exact type of instruments. A stringent calibration, characterization and quality control was applied on all the data by the person in charge of the measurements (following IDMP recommendations, CIE 1994), the coherence of the data was verified by the author. The list of the stations is given on Table I.

Meteosat sites	climate	period	latitude °	longitude °	altitude m	operated by
Berlin Dahlem (D)		1980-2009	52.46	13.3	58	
Bratislava (SK)		1994-2007	48.17	17.08	195	CIE - ICA
Carpentras (F)	mediterranean	1990-2010	44.08	5.06	100	BSRN - Météo France
Davos Dorf (CH)	semi-continental alpin	1981-2010	46.81	9.84	1610	WRDC - Met Office
El Saler (Spain)	semi arid	1999-2006	39.35	-0.32	10	FluxNet
Geneva (CH)	semi-continental	1980-2010	46.20	6.13	420	CIE - UNIGE
Ilorin (Nigeria)	equatorial desert	1993-2005	8.53	4.57	350	BSRN
Lindenberg (D)	moderate maritime	1995-2004	52.22	14.12	125	BSRN - DWD
Locarno Monti (CH)		1981-2010	46.17	8.78	367	ANETZ - Météo Suisse
Murcia San-Javier (Spain)	semi arid	1985-2008	37.78	-0.82	3	
Nantes (F)	oceanic	1995-2007	47.15	-1.33	30	CIE - CSTB
Payerne (CH)	moderate maritime/continental	1981-2010	46.82	6.95	490	BSRN - Météo Suisse
Sion (CH)	dry alpine	1981-2010	46.22	7.33	489	ANETZ - Météo Suisse
Sonnblick (A)	temperate alpine	1994-2009	47.05	12.95	3105	WRDC - ZAMG
Tamanrasset (Algeria)	hot, dry desert	1995-2010	22.78	5.52	1400	BSRN - Met Office
Thessaloniki (GR)	mediterranean temperate	1993-2006	40.63	22.97	60	WRDC - Met Office
Toravere (Estonia)	cold humid	1999-2010	58.27	26.47	70	BSRN - EMHI
Valentia (Ireland)	temperate maritime	1996-2009	51.93	-10.25	14	WRDC - Met Office
Vaulx-en-Velin (F)	semi-continental	1994-2010	45.78	4.93	170	CIE - ENTPE
Wien / Hohe Warte (A)	continental	1994-2009	48.25	16.35	203	WRDC - ZAMG
Zürich Kloten (CH)	temperate atlantic	1981-2010	47.38	8.57	558	ANETZ - Météo Suisse
Bondville (IL)		1995-2008	40.05	-88.37	213	SurfRad - NREL
Desert Rock (NV)	desert	1999-2008	36.62	-116.02	1007	SurfRad - NREL
Fort Peck (MO)		1995-2008	48.31	-105.10	634	SurfRad - NREL
Goodwin Creek (MI)		1995-2008	34.25	-89.87	98	SurfRad - NREL
Penn State (PY)		1999-2008	40.72	-77.93	376	SurfRad - NREL
Table Mountain (CO)	semi-arid	1996-2008	40.13	-105.24	1689	SurfRad - NREL

ANETZ	Automatisches meteorologisches Mess-und Beobachtungsnetz	ENTPE	Ecole Nationale des Mines de Paris
BSRN	Baseline Surface Radiation Network	UNIGE	University of Geneva
CIE	Commission Internationale pour l'Eclairage	WRDC	World Radiation Data Center
CSTB	Centre Scientifique et Technique du Bâtiment	ZAMG	Zentralanstalt für Meteorologie und Geophysik
DWD	Deutscher Wetterdienst		
EMHI	The Estonian Meteorological and Hydrological Institute	NREL	National Renewable Energy Laboratory
ICA	Institute of Construction and Architecture, Slovak Academy of Sciences	SurfRad	Surface Radiation Network

Table 1: Ground sites list

3. Ground data accuracy

Sensor calibration is the key point for precise acquisition in the field of solar radiation. The radiation sensors should be calibrated by comparison against a sub-standard before the beginning of the acquisition period, and then every year. Due to the possible errors and inaccuracies, a post-calibration is difficult to conduct.

The quality control is the first step in the process of using ground data. It detects significant instrumental errors like calibration, orientation, leveling, coherence, etc. An automatic quality control cannot detect all the acquisition inaccuracies, one of the remaining points to be assessed is the sensors' calibration coefficient used to convert the acquired data into physical values. This can only be done by comparison of redundant or complementary data.

The sensors' calibration coefficient can be verified for clear sky conditions by comparison. Day by day, the highest hourly value is selected from the measurements and plotted against the day of the year as illustrated on Figure 1. These points are representative of the clearest conditions within the considered day. As the highest value for each day is selected, the upper limit represents the clear sky conditions. On Figure 2, the clearness index K_t (global irradiance G normalized by the corresponding extra-atmospheric irradiance I_o) is plotted against the solar elevation angle in hourly values. Here again, two different data sets are represented; the upper limits of the two data sets should lie together if the calibration is coherent. On such graphs, data from different sites or different year for the same site can be compared.

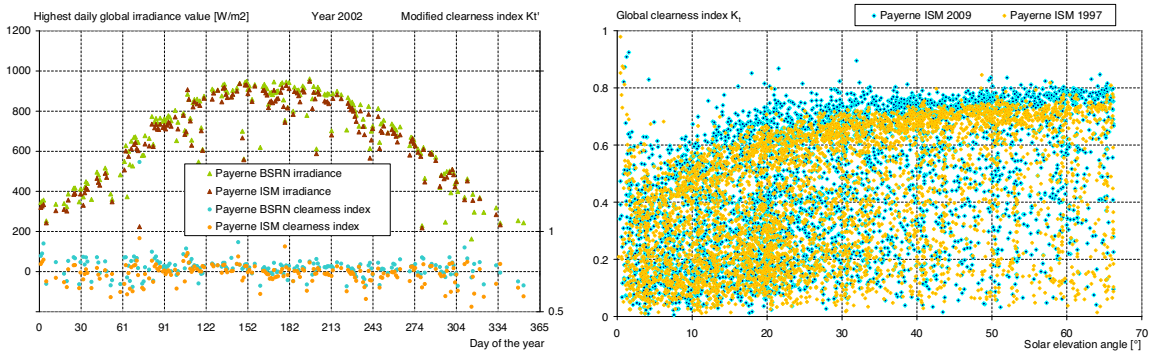

Figure 1 (left): highest daily global irradiance value versus the day of the year for two different data sets.
Figure 2 (right): clearness index versus the solar elevation angle for the same site and two different years.

When the atmospheric aerosol optical depth (*aod*) and the water vapor column (w) for the site are known, from an independent network such as aeronet, the sensors' calibration can be assessed by comparison with the help of a clear sky model. On such networks, the aerosol optical depth is acquired as soon as direct sun is present; the values are then averaged to give a daily value. The water vapor w is evaluated from the ground temperature (T_a) and relative humidity (HR) by the use of a model such as Atwater model (Atwater 1976). When the temperature and humidity measurements are missing, the data from a neighboring station (if applicable) can be used; the water vapor can also be retrieved from the aeronet network. These *aod* and w values are then used with the Solis clear sky model (Muller 2004, Ineichen 2008a) to evaluate clear sky hourly G and G_b values and plotted on same graphs than above.

If none of the above method can be applied, the results issued from the use of such data bank should be taken with caution.

4. Derived data

Two different derived data sets are analyzed in this study: average and typical years derived from long-term measurements, and specific years derived hour by hour from satellite images. These two categories of products will be compared separately against the corresponding ground data sets.

3.1. Average and typical years

These sets of data are obtained from 10 to 20 years of measurements, and partially interpolated between

stations. Some of them are corrected with the help of satellite images. For Switzerland and the United States, Design Reference Year (DRY from EMPA, CH) and Typical Meteorological Year (TMY from NREL, USA) are also part of the comparison.

These data are derived within the following networks, programs or softwares:

- PVGIS: Photovoltaic Geographical Information System provides a map-based inventory of solar energy resource and assessment of the electricity generation from photovoltaic systems in Europe, Africa, and South-West Asia (available from http://re.jrc.ec.europa.eu/pvgis/). For Europe, a new data set is available in version 4, evaluated by Eumetsat climate satellite facilities (CMSAF, DWD).
- WRDC: the World Radiation Data Centre Online Archive contains international solar radiation data stored at the WRDC, which is a central depository for data collected over one thousand measurement sites throughout the world (available from http://wrdc-mgo.nrel.gov/).
- RetScreen: the RETScreen Clean Energy Project Analysis Software is a unique decision support tool developed with the contribution of numerous experts from government, industry, and academia. The software, provided free-of-charge, can be used worldwide to evaluate the energy production and savings, costs, emission reductions, financial viability and risk for various types of Renewable-energy and Energy-efficient Technologies (RETs, available from http://www.retscreen.net).
- NASA SSE is a renewable energy resource web site of global meteorology and surface solar energy climatology from NASA satellite data on 1 by 1 degree resolution (available from http://eosweb.larc.nasa.gov/sse/).
- EMPClimate: this database contains monthly means of solar irradiation (downwelling shortwave irradiation), minima, maxima and mean values of air temperature at 2 m, minima, maxima and mean values of relative humidity at 2 m and covers the whole world. It has been created by data fusion techniques applied to satellite data, meteorological re-analyses from the National Centers for Environmental Prediction and the National Center for Atmospheric Research (NCEP /NCAR USA) and orography for the period 1990-2004 by Mines ParisTech (available from the MeSor[1] portal at http://www.mesor.org).
- Meteonorm is a comprehensive meteorological reference software, incorporating a catalogue of meteorological data and calculation procedures for solar applications and system design at any desired location in the world. It is based on over 23 years of experience in the development of meteorological databases for energy applications (see http://www.meteonorm.com).
- EMPA DRY and NASA TMY: Design Reference Year and Typical Reference Year contain hourly climate data for a specific location, arranged as hourly sets of simultaneous climate parameters. The basic requirements for a DRY or a TRY are that it correspond to an average year, both regarding monthly or seasonal mean values, occurrence and persistence of warm, cold, sunny or overcast periods.
- ESRA: the European Solar Radiation Atlas is oriented towards the needs of the users like solar architects and engineers, respecting the state of the art of their working field and their need of precise input data. From best available measured solar data complemented with other meteorological data necessary for solar engineering, digital maps for the European continents are produced. Satellite-derived maps help in improving accuracy in spatial interpolation (see http://www.helioclim.com).
- Satel-Light is a Meteosat image based data server developed within a Joule XII European project that provides 5 years of half hourly data of solar irradiance and daylight components with a spatial

[1] MeSor: Management and Exploitation of Solar Resource Knowledge. The MeSor project is a European funded Coordination Action which aims at removing the uncertainty and improving the management of the solar energy resource knowledge. The project includes activities in user guidance (benchmarking of models and data sets; development of a handbook on best practices on how to use solar resource data), unification of access to information (use of advanced information technologies; offering one-stop-access to several databases), connecting to other initiatives (INSPIRE of the EU, POWER of the NASA, SHC and PVPS of the IEA, GMES/GEO) and to related scientific communities (energy, meteorology, geography, medicine, ecology), and dissemination (stakeholders involvement, future R&D, communication).

resolution of 10 km by 10 km. It covers all Europe and part of North Africa (available from http://www.satel-light.com). The average over the years 1996 to 2000 is used here.

- SolarGis from GeoModel: a modified Heliosat-2 algorithm is used to calculate irradiance from 15-minute MSG data, adapted for multispectral MSG data, with improvements of snow classification and cloud index determination and a terrain disaggregation (see http://www.geomodel.eu and below)

3.2. Specific satellite derived years

The second set of data is obtained from satellite images, and is representative of data for specific years:

- The Helioclim-3 data bank (http://www.soda-is.com) is produced with the Heliosat-2 method that converts observations made by geostationary meteorological satellites into estimates of the global irradiation at ground level. This version integrates the knowledge gained by various exploitations of the original Heliosat method and its varieties in a coherent and thorough way.
  It is based upon the same physical principles, but the inputs to the method are calibrated radiances, instead of the digital counts output from the sensor. This change opens the possibilities of using known models of the physical processes in atmospheric optics, thus removing the need for empirically defined parameters and of pyranometric measurements to tune them. The ESRA models (ESRA 2000, Rigollier 2000 and 2004) are used for modeling the clear-sky irradiation. The assessment of the ground albedo and the cloud albedo is based upon explicit formulations of the path radiance and the transmittance of the atmosphere. The turbidity is based on climatic monthly Linke Turbidity coefficients data banks.

- SolarGis (http://www.geomodel.eu): the irradiance components are the results of a five steps process: a multi-spectral analysis classifies the pixels (normalized difference snow index (Ruyter 2007), cloud index (Derrien 2005), and temporal variability index), the lower boundary (LB) evaluation is done for each time slot (based on the original approach by Perez (2002)), a spatial variability is introduced for the upper boundary (UP) and the cloud index definition, the Solis clear sky model is used as normalization [simplified version (Ineichen 2008a), as inputs, the climatology values from the NVAP water vapor database (Randl 1996) and Atmospheric Optical Depth data by (Remund 2008) assimilated with Aeronet and Aerocom datasets are used], and a terrain disaggregation is finally applied [based on the approach by Ruiz-Arias (2010), with a spatial resolution of 100 m].

- Satel-Light (http://www.satel-light.com): the only parameter directly computed from the satellite image is the global horizontal irradiance. All other parameters are computed from it. The global horizontal irradiance is estimated from the pixel value of the satellite image using the concept of the Heliosat method, proposed by Cano (Cano, 1986). This method was modified by Beyer (Beyer, 1996) and further improvements have been made to it for Satel-Light. The Heliosat method is based on the assumption that the albedo of a cloudy atmosphere will usually be larger than the albedo of the ocean or the earth surface (this is not true if the ground is covered with snow). Thus, the increase of the albedo gives a measure of the cloud cover. Then, the albedo is used to compute the cloud index, which is representative of the cloud cover.
  The presence of snow increases significantly the albedo, making the detection of cloudless situations almost impossible when using only the satellite visible channel. Unfortunately, the generation of Meteosat satellites used at the time of the project did not offer channels which could be used to make the distinction between snow cover and cloud cover. This means that a pixel overlooking an area covered with snow during part of the month is considered as a pixel overlooking an area covered with clouds during that same period of time. The solar radiation for this pixel will then be underestimated (Ineichen 1999).

- Suny model (State University of New York at Albany): the semi-empirical model producing global Irradiance (G) and direct irradiance (G_b) from geostationary satellite images (visible channel) has been described in detail in two previous articles (Perez 2002, Perez 2003).
  The cloud index determination is individualized for each ground (pixel) location. It is determined

from the location-specific relative normalized pixel brightness -- i.e., the brightness of a pixel in relation to its maximum and minimum possible value, the latter representing clear conditions (brightness of ground) and the former representing cloudy conditions (brightness of thick cloud top). Because it is individualized for each pixel, this process accounts for ground reflectivity differences over space and time and does not require an absolute knowledge of satellite sensors calibration. The model also accounts for site-specific ground bi-directional (specular) reflectance characteristics and for snow cover when present (Perez 2002, Perez 2003).

The clear sky envelopes (Bird model adapted by Maxwell 1998) represent the upper limit of irradiances generated by the model. These envelopes are functions of ground elevation and atmospheric turbidity as quantified by atmospheric precipitable water w and by atmospheric optical depth (*aod*). In its operational version, the model uses monthly site/specific climatological estimates of *w* and broad-band *aod* traceable to (Randal 1996, Mischenko 1999, Yu 2003).

The model enhances its performance in complex terrains, via a systematic internal calibration of its output to modeled clear sky profiles (Perez 2003).

5. Evaluation method

A reference period covering the years 1999 to 2006 will guide the evaluation of the products. The average yearly total *H* is determined by the mean value over the reference period and is used as normalization for the yearly totals. This normalized average (=100%) is represented on the Figure 3 by the first blue bar from the left and labeled 1999-2006 average. The corresponding 100% dashed line is surrounded by ± one standard deviation (estimated over the 8 years of the reference period) in light orange on the graph. The following values are given on the Figure 3:

(1) first left blue bar: average annual irradiation on the reference period (1999-2006 => 100%),

(2) blue bars: relative annual ground measurements,

(3) yellow bars: average data banks, satellite based or average ground measurements,

(4) orange bars: year by year SolarGis irradiation (European sites),

(5) green bars: year by year Helioclim 3 irradiation (European sites),

(6) light blue bars: year by year Satel-Light data for the 1996 to 2000 period (European sites),

(7) grey bars: year by year Suny irradiation (for United States sites),

(8) red bars: average data banks annual deviation from the 1999-2006 reference average,

(9) brown bars: ground measurements annual deviation from the 1999-2006 reference average.

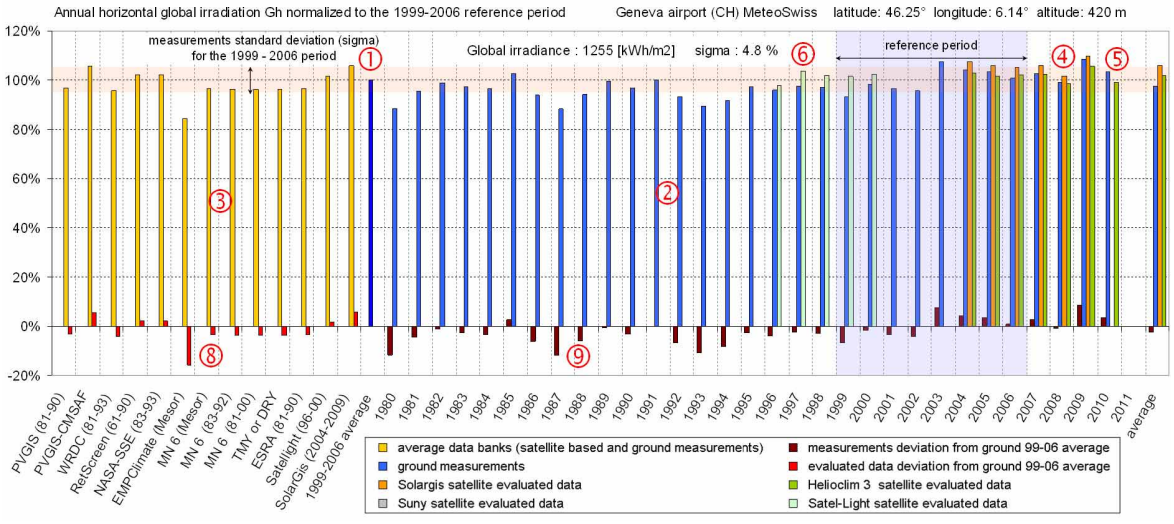

Figure 3: Relative total annual irradiation normalized to the average annual value over the reference period (1999-2006) for the site of Geneva airport. The mean bias deviation is also given.

Table II: Variability of the annual total global irradiance, and deviation from the reference average.

		1999-2006 average		1981	1982	1983	1984	1985	1986	1987	1988	1989	1990	1991	1992	1993	1994	1995	1996	1997	1998	1999	2000	2001	2002	2003	2004	2005	2006	2007	2008	2009	2010	whole period average
				reference period																														
Berlin Dahlem (D)	Yearly total [kWh/m^2]	1058	Yearly total [kWh/m^2]	903	1080	964	926	965	968	934	1003	1089	1055	970	993	960	1008	1037	938	1063	960	1039	1006	958	1013	1187	1034	1114	1112	1080	1079	1112		1016
	fluctuation [%]	7%	deviation from average	-15%	2%	-9%	-12%	-9%	-8%	-12%	-5%	3%	0%	-8%	-6%	-9%	-5%	-2%	-11%	0%	-9%	-2%	-5%	-9%	-4%	12%	-2%	5%	5%	2%	2%	5%		-4%
Bratislava (Slovakia)	Yearly total [kWh/m^2]	1172	Yearly total [kWh/m^2]														1159	1105	1099	1173	1142	1138	1208	1141	1150	1249	1131	1180	1182	1212				1162
	fluctuation [%]	3%	deviation from average														-1%	-6%	-6%	0%	-3%	-3%	3%	-3%	-2%	7%	-4%	1%	1%	3%				-1%
Carpentras (F)	Yearly total [kWh/m^2]	1581	Yearly total [kWh/m^2]	1521									1558	1569	1487	1510	1538	1575		1555	1619	1539	1556	1586	1551	1612	1595	1596	1613	1594	1522	1619	1569	1566
	fluctuation [%]	2%	deviation from average	-4%									-1%	-1%	-6%	-4%	-3%	0%		-2%	2%	-3%	-2%	0%	-2%	2%	1%	1%	2%	1%	-4%	2%	-1%	-1%
Davos (CH)	Yearly total [kWh/m^2]	1344	Yearly total [kWh/m^2]	1327	1367	1373	1391	1442	1414	1285	1296	1279	1237	1349	1328	1304	1298	1297	1367	1376	1346	1323	1319	1332	1312	1448	1344	1338	1337	1373	1400	1401	1332	1301
	fluctuation [%]	3%	deviation from average	-1%	2%	2%	3%	7%	5%	-4%	-4%	-5%	-8%	0%	-1%	-3%	-3%	-3%	2%	2%	0%	-2%	-2%	-1%	-2%	8%	0%	0%	-1%	2%	4%	4%	-1%	-3%
El Saler (ES)	Yearly total [kWh/m^2]	1652	Yearly total [kWh/m^2]																			1615	1668	1704	1623	1620	1614	1680	1696					1652
	fluctuation [%]	2%	deviation from average																			-2%	1%	3%	-2%	-2%	-2%	2%	3%					0%
Geneva CIE (CH)	Yearly total [kWh/m^2]	1269	Yearly total [kWh/m^2]										1275	1249	1206	1177	1152	1219	1213	1275	1294	1215	1224	1260	1249	1349	1276	1305	1273	1292	1260	1326	1238	1254
	fluctuation [%]	3%	deviation from average										0%	-2%	-5%	-7%	-9%	-4%	-4%	1%	2%	-4%	-4%	-1%	-2%	6%	1%	3%	0%	2%	-1%	5%	-2%	-1%
Geneva ISM (CH)	Yearly total [kWh/m^2]	1279	Yearly total [kWh/m^2]	1247	1292	1269	1261	1341	1225	1152	1228	1299	1265	1304	1218	1166	1196	1272	1254	1273	1268	1220	1285	1260	1249	1350	1308	1297	1265	1289	1244	1361	1298	1262
	fluctuation [%]	3%	deviation from average	-3%	1%	-1%	-1%	5%	-4%	-10%	-4%	2%	-1%	2%	-5%	-9%	-6%	-1%	-2%	-1%	-1%	-5%	0%	-1%	-2%	6%	2%	1%	-1%	1%	-3%	6%	1%	-1%
Lindenberg (D)	Yearly total [kWh/m^2]	1082	Yearly total [kWh/m^2]															1100	1040	1130	1045	1110	1060	1026	1036	1190	1071							1081
	fluctuation [%]	4%	deviation from average															2%	-4%	4%	-3%	3%	-2%	-5%	-4%	10%	-1%							0%
Locarno (CH)	Yearly total [kWh/m^2]	1312	Yearly total [kWh/m^2]	1226	1263	1206	1215	1268	1208	1277	1236	1311	1327	1355	1221	1263	1266	1333	1298	1367	1302	1251	1239	1322	1286	1411	1261	1411	1313	1441	1333	1443	1336	1300
	fluctuation [%]	5%	deviation from average	-7%	-4%	-8%	-7%	-3%	-8%	-3%	-6%	0%	1%	3%	-7%	-4%	-4%	2%	-1%	4%	-1%	-5%	-6%	1%	-2%	8%	-4%	8%	0%	10%	2%	10%	2%	-1%
Murcia (ES)	Yearly total [kWh/m^2]	1727	Yearly total [kWh/m^2]					1702	1686	1696	1726	1668	1697	1705	1655	1700	1726	1724	1737	1749	1742	1735	1770	1748	1664	1683	1696	1781	1740	1746	1779			1719
	fluctuation [%]	2%	deviation from average					-1%	-2%	-2%	0%	-3%	-2%	-1%	-4%	-2%	0%	0%	1%	1%	1%	0%	2%	1%	-4%	-3%	-2%	3%	1%	1%	3%			0%
Nantes (F)	Yearly total [kWh/m^2]	1252	Yearly total [kWh/m^2]															1242	1263	1295	1204	1201	1187	1231	1239	1315	1293	1302	1249	1209	1229		1313	1251
	fluctuation [%]	4%	deviation from average															-1%	1%	3%	-4%	-4%	-5%	-2%	-1%	5%	3%	4%	0%	-3%	-2%		5%	0%
Payerne ISM (CH)	Yearly total [kWh/m^2]	1260	Yearly total [kWh/m^2]	1271	1314	1290	1216	1287	1237	1165	1220	1266	1300	1282	1232	1211	1145	1235	1216	1263	1244	1185	1262	1199	1201	1372	1263	1269	1248	1288	1238	1338	1274	1251
	fluctuation [%]	4%	deviation from average	2%	5%	3%	-3%	3%	-1%	-7%	-2%	1%	4%	3%	-1%	-3%	-8%	-1%	-3%	1%	0%	-5%	1%	-4%	-4%	10%	1%	2%	0%	3%	-1%	7%	2%	0%
Payerne BSRN (CH)	Yearly total [kWh/m^2]	1250	Yearly total [kWh/m^2]													1193	1179	1252	1170	1234	1272	1192	1265	1217	1220	1373	1261	1294	1257	1302	1238	1316		1249
	fluctuation [%]	5%	deviation from average													-5%	-6%	-1%	-7%	-2%	1%	-5%	0%	-3%	-3%	9%	0%	3%	0%	3%	-2%	4%		-1%
Sion (CH)	Yearly total [kWh/m^2]	1355	Yearly total [kWh/m^2]	1272	1335	1288	1314	1359	1325	1261	1290	1362	1356	1365	1300	1511	1373	1366	1326	1397	1375	1282	1336	1340	1320	1412	1356	1385	1406	1421	1444	1469	1432	1315
	fluctuation [%]	3%	deviation from average	-6%	-1%	-5%	-3%	0%	-2%	-7%	-5%	1%	0%	1%	-4%	12%	1%	1%	-2%	3%	2%	-5%	-1%	-1%	-3%	4%	0%	2%	4%	5%	7%	8%	6%	-3%
Sonnblick (A)	Yearly total [kWh/m^2]	1490	Yearly total [kWh/m^2]														1500	1512	1508	1522	1463	1408	1496	1529	1474	1570	1483	1488	1469	1447	1461	1456		1487
	fluctuation [%]	3%	deviation from average														1%	2%	1%	2%	-2%	-5%	0%	3%	-1%	5%	0%	0%	-1%	-3%	-2%	-2%		0%
Tamanrasset (Algeria)	Yearly total [kWh/m^2]	2353	Yearly total [kWh/m^2]															2206	2278	2250	2228	2403	2336	2458	2343	2336	2369	2285	2291	2388	2385	2336	2361	2328
	fluctuation [%]	2%	deviation from average															-6%	-3%	-4%	-5%	2%	-1%	4%	0%	-1%	1%	-3%	-3%	1%	1%	-1%	0%	-1%
Thessaloniki (GR)	Yearly total [kWh/m^2]	1580	Yearly total [kWh/m^2]													1578	1538	1554	1429	1547	1549	1569	1651	1580	1513	1580	1555	1613	1579					1560
	fluctuation [%]	3%	deviation from average													0%	-3%	-2%	-10%	-2%	-2%	-1%	4%	0%	-4%	0%	-2%	2%	0%					-1%
Toravere (Estonia)	Yearly total [kWh/m^2]	997	Yearly total [kWh/m^2]																			1068	938	965	1072	927	951	1020	1034	991	927	967	975	986
	fluctuation [%]	6%	deviation from average																			7%	-6%	-3%	8%	-7%	-5%	2%	4%	-1%	-7%	-3%	-2%	-1%
Vaulx-en-Velin (F)	Yearly total [kWh/m^2]	1316	Yearly total [kWh/m^2]													1174	1245	1325	1271	1286	1392	1293	1345	1297	1262	1386	1247	1354	1341	1273	1212	1317	1257	1293
	fluctuation [%]	4%	deviation from average													-11%	-5%	1%	-3%	-2%	6%	-2%	2%	-1%	-4%	5%	-5%	3%	2%	-3%	-8%	0%	-4%	-2%
Wien (A)	Yearly total [kWh/m^2]	1215	Yearly total [kWh/m^2]														1234	1161	1138	1239	1200	1187	1259	1173	1240	1349	1131	1160	1223	1190	1176	1198		1204
	fluctuation [%]	6%	deviation from average														2%	-4%	-6%	2%	-1%	-2%	4%	-3%	2%	11%	-7%	-5%	1%	-2%	-3%	-1%		-1%
Zürich (CH)	Yearly total [kWh/m^2]	1134	Yearly total [kWh/m^2]	1095	1064	1137	1107	1117	1095	1040	1118	1148	1180	1086	1037	1054	1034	1071	1104	1162	1095	1019	1079	1063	1085	1263	1184	1218	1165	1221	1142	1239	1177	1084
	fluctuation [%]	7%	deviation from average	-4%	-6%	0%	-2%	-2%	-3%	-8%	-1%	1%	4%	-4%	-9%	-7%	-9%	-6%	-3%	2%	-3%	-10%	-5%	-6%	-4%	11%	4%	7%	3%	8%	1%	9%	4%	-4%

6. Results

5.1. Interannual variability

The interannual variability of the global irradiation *H* for the European stations is given on Table II. The reference period average, mean bias difference and fluctuation (root mean square difference) values are given in the most left column, while the values over the whole measurements period are given in the most right column.

The first established fact is that even if the standard deviations don't exceed some percents, specific years can be more that 10% away from the average.

The European sites can be separated in 2 groups. For some stations, there is a tendency to have higher yearly total global irradiation in the last years, while a diminution can be seen for other sites. This is illustrated on figure 4 where a 14 year reference sequence (1996-2009) is used for normalization. The opposite tendency can clearly be seen on data from Geneva and Berlin, and from Vaulx-en-Velin for example. For Geneva and Vaulx-en-Velin, with relatively similar climates and situated at only 100 km one from the other, this cannot be attributed to a regional effect, but can come from a turbidity change that could not be investigated due to a lack of aerosol optical depth knowledge.

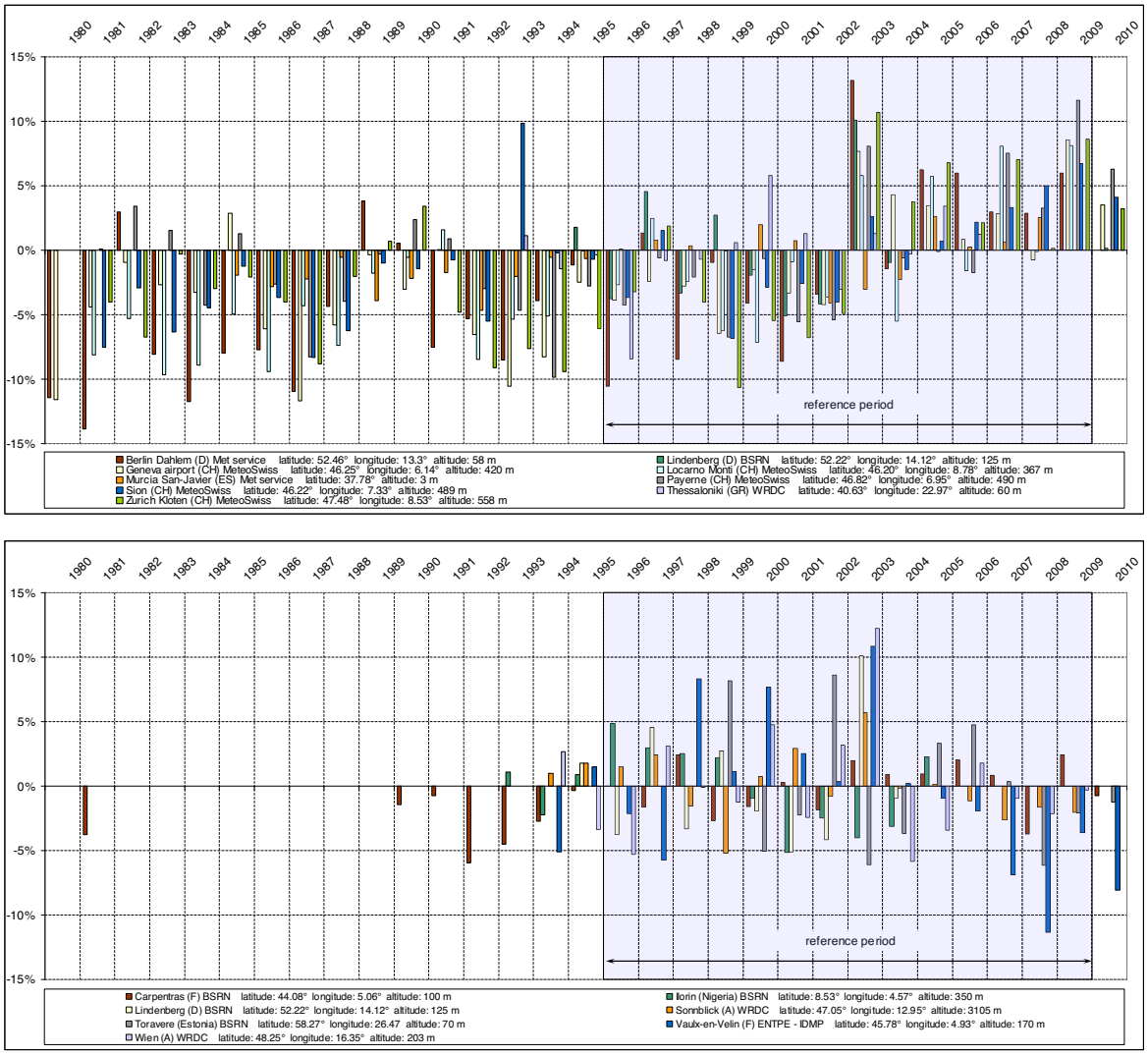

Figure 4: Yearly total global irradiation deviation from the 1996 to 2009 average for two groups of sites.

For two sites, Payerne and Geneva, two specific data sets are acquired and can be compared. In Geneva, the ISM (MeteoSwiss) site is situated at the Geneva airport, while the CIE station is situated in the center of the city, i.e. at five kilometers from the airport. In Payerne, the two stations are on the same site and operated by MeteoSwiss. Looking at Figure 5 where the annual total global irradiation *H* is plotted versus the year,

important differences can be seen between the two Geneva and the two Payerne data sets. If the general tendency is the same for all the curves, there are significant differences, not always of the same sign. This has to be underlined, particularly for the site of Payerne where the acquisition is done side by side; the difference can be attributed to the sensors' calibration. These two data sets are analyzed and corrected following section 3.

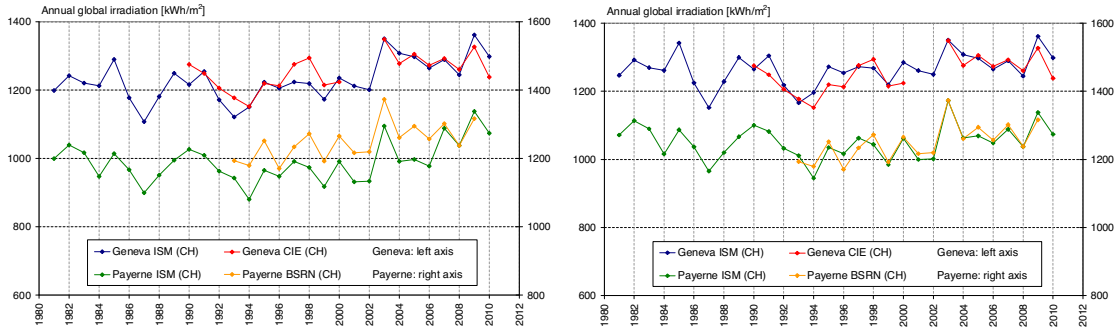

Figure 5: Total annual global irradiation for the two data sets of Geneva and Payerne before and after correction.

5.2. Average and typical years

EMP Climate obtained from the MeSor portal is a prototype; the results are highly variable, and, even if given on the graphs and in the Tables, the values should not be used.

For Meteonorm, three different possibilities are investigated: monthly values obtained from the MeSor portal (http://www.mesor.org), product based on average ground measurements acquired from 1983 to 1992, and over a longer period, i.e. from 1981 to 2000. The results are very similar for all the Meteonorm products.

It can be seen on Figure 3 for the site of Geneva that except for EMPClimate (see above remark), the different products give values near or within ± one standard deviation around the considered reference period. The evaluated products can therefore be used with a good precision for photovoltaic power plant sizing (only the annual total is relevant in that case).

On Figure 6, the seasonal evolution of the monthly global irradiation obtained from the different products is represented for the site of Payerne, data from the BSRN network. In most of the cases, when a model over- or underestimates the irradiation, it does it over the whole year, i.e. the bias is not linked to a seasonal effect as for example the albedo variation.

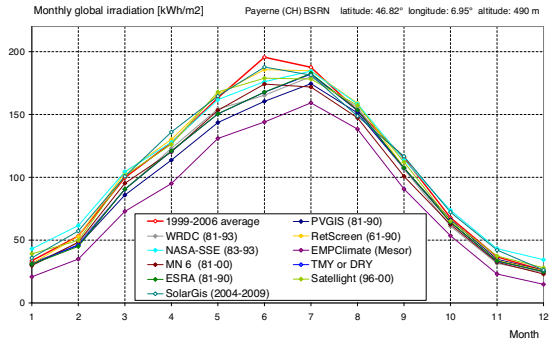

Figure 6: Seasonal evolution of the monthly global irradiation for the site of Payerne.

The results for the European sites and the average products are given in Table III, where the deviation from the average over the reference period is given in absolute and relative values. In the first column, the1999-2006 average is given with its the standard deviation over the. The results for the products that are within ± one standard deviation over the reference period are given in blue in the Table. The corresponding Table for the stations situated in the United States can be found in the Annex on http://www.cuepe.ch.

5.3. Specific satellite derived years

Over Europe, Satel-Light data are evaluated from 1996 to 2000, Helioclim 3 and SolarGis products are

		1999-2006 average		PVGIS (81-90)	PVGIS-CMSAF	WRDC (81-93)	RetScreen (61-90)	NASA-SSE (83-93)	EMPClimate (Mesor)	MN 6 (Mesor)	MN 6 (83-92)	MN 6 (81-00)	TMY or DRY	ESRA (81-90)	Satellight (96-00)	SolarGis (2004-2009)
		average data														
Berlin Dahlem (D)	Yearly total [kWh/m2]	1058		997	1053	988	1000	1000	743	1003		1021		974	1044	
	fluctuation [kWh/m2]	74	Deviation	-61	-4	-70	-58	-58	-315	-55		-37		-84	-14	
	fluctuation [%]	7%	from average	-6%	0%	-7%	-6%	-6%	-30%	-5%		-3%		-8%	-1%	
Bratislava (Slovakia)	Yearly total [kWh/m^2]	1172		1170	1214	1188	1190	1165	1204	1183	1214	1190		1227	1197	1195
	fluctuation [kWh/m^2]	41	Deviation	-2	41	16	17	-7	32	11	42	18		55	25	23
	fluctuation [%]	3%	from average	0%	4%	1%	1%	-1%	3%	1%	4%	2%		5%	2%	2%
Carpentras (F)	Yearly total [kWh/m^2]	1581		1492	1626	1511	1348	1491	1352	1520	1504	1522		1501	1599	1599
	fluctuation [kWh/m^2]	29	Deviation	-89	45	-70	-232	-90	-228	-61	-77	-59		-80	18	18
	fluctuation [%]	2%	from average	-6%	3%	-4%	-15%	-6%	-14%	-4%	-5%	-4%		-5%	1%	1%
Davos (CH)	Yearly total [kWh/m^2]	1344		1296	1156	1334	1371	1274	1022	1478	1405	1405	1339	1343	1141	1290
	fluctuation [kWh/m^2]	43	Deviation	-48	-188	-10	27	-70	-322	134	61	61	-5	-1	-203	-54
	fluctuation [%]	3%	from average	-4%	-14%	-1%	2%	-5%	-24%	10%	5%	5%	0%	0%	-15%	-4%
El Saler (ES)	Yearly total [kWh/m^2]	1652		1525	1748	1724	1642	1820	1575	1677	1615	1616		1730	1665	1699
	fluctuation [kWh/m^2]	38	Deviation	-127	95	72	-10	168	-78	24	-37	-36		78	13	46
	fluctuation [%]	2%	from average	-8%	6%	4%	-1%	10%	-5%	1%	-2%	-2%		5%	1%	3%
Geneva CIE (CH)	Yearly total [kWh/m^2]	1269		1215	1326	1201	1283	1283	1057	1211	1209	1208	1207	1211	1277	1327
	fluctuation [kWh/m^2]	43	Deviation	-54	57	-67	14	14	-212	-58	-59	-60	-62	-58	8	58
	fluctuation [%]	3%	from average	-4%	5%	-5%	1%	1%	-17%	-5%	-5%	-5%	-5%	-5%	1%	5%
Geneva ISM (CH)	Yearly total [kWh/m^2]	1279		1215	1326	1201	1283	1283	1057	1211	1209	1208	1207	1211	1277	1327
	fluctuation [kWh/m^2]	40	Deviation	-64	47	-78	4	4	-222	-69	-70	-71	-73	-69	-2	48
	fluctuation [%]	3%	from average	-5%	4%	-6%	0%	0%	-17%	-5%	-5%	-6%	-6%	-5%	0%	4%
Lindenberg (D)	Yearly total [kWh/m2]	1082		1013	1079	1077	1077	1011	1028	1002	1070	1070		982	1070	1040
	fluctuation [kWh/m2]	39	Deviation	-69	-3	-5	-5	-71	-54	-80	-12	-12		-100	-12	-42
	fluctuation [%]	4%	from average	-6%	0%	0%	0%	-7%	-5%	-7%	-1%	-1%		-9%	-1%	-4%
Locarno (CH)	Yearly total [kWh/m2]	1312		1215	1341	1201	1283	1283	1057	1211	1209	1208	1207	1211	1266	1370
	fluctuation [kWh/m2]	68	Deviation	-97	30	-110	-29	-29	-254	-101	-102	-103	-105	-101	-45	58
	fluctuation [%]	5%	from average	-7%	2%	-8%	-2%	-2%	-19%	-8%	-8%	-8%	-8%	-8%	-3%	4%
Murcia (ES)	Yearly total [kWh/m^2]	1727		1697	1844	1724	1750	1846	1748	1734	1734	1734		1730	1858	
	fluctuation [kWh/m^2]	42	Deviation	-30	117	-3	23	119	21	7	7	7		3	131	
	fluctuation [%]	2%	from average	-2%	7%	0%	1%	7%	1%	0%	0%	0%		0%	8%	
Nantes (F)	Yearly total [kWh/m^2]	1252		1231	1284	1200	1223	1181	1111	1226	1219	1226		1256	1231	1206
	fluctuation [kWh/m^2]	47	Deviation	-21	32	-52	-29	-71	-141	-26	-33	-26		4	-21	-46
	fluctuation [%]	4%	from average	-2%	3%	-4%	-2%	-6%	-11%	-2%	-3%	-2%		0%	-2%	-4%
Payerne BSRN (CH)	Yearly total [kWh/m^2]	1260		1141	1300	1170	1245	1283	978	1167	1173	1159	1172	1172	1242	1270
	fluctuation [kWh/m^2]	56	Deviation	-118	40	-89	-14	23	-281	-92	-86	-101	-88	-88	-18	10
	fluctuation [%]	4%	from average	-9%	3%	-7%	-1%	2%	-22%	-7%	-7%	-8%	-7%	-7%	-1%	1%
Payerne ISM (CH)	Yearly total [kWh/m^2]	1250		1141	1300	1170	1245	1283	978	1167	1173	1159	1172	1172	1242	1270
	fluctuation [kWh/m^2]	60	Deviation	-109	50	-79	-4	33	-271	-83	-77	-91	-78	-78	-8	20
	fluctuation [%]	5%	from average	-9%	4%	-6%	0%	3%	-22%	-7%	-6%	-7%	-6%	-6%	-1%	2%
Sion (CH)	Yearly total [kWh/m^2]	1355		1371	1329		1283	1283	1052	1287	1395	1395	1314	1298	1400	1357
	fluctuation [kWh/m^2]	45	Deviation	16	-25		-71	-71	-303	-67	40	40	-40	-57	45	3
	fluctuation [%]	3%	from average	1%	-2%		-5%	-5%	-22%	-5%	3%	3%	-3%	-4%	3%	0%
Sonnblick (A)	Yearly total [kWh/m^2]	1490		1300	1022	1373	1390		1057	1211	1381	1410		1412	1173	1372
	fluctuation [kWh/m^2]	47	Deviation	-190	-468	-116	-100		-432	-279	-108	-80		-78	-317	-118
	fluctuation [%]	3%	from average	-13%	-31%	-8%	-7%		-29%	-19%	-7%	-5%		-5%	-21%	-8%
Tamanrasset (Algeria)	Yearly total [kWh/m^2]	2353		2372	2363	2363	2407	2154	2878	2365	2365	2365				2333
	fluctuation [kWh/m^2]	57	Deviation	19	10	10	54	-198	525	13	12	12				-20
	fluctuation [%]	2%	from average	1%	0%	0%	2%	-8%	22%	1%	1%	1%				-1%
Thessaloniki (GR)	Yearly total [kWh/m^2]	1580		1436	1659	1117	1476	1476	1309	1523	1209	1493		1447	1520	1580
	fluctuation [kWh/m^2]	40	Deviation	-145	79	-463	-105	-105	-271	-57	-371	-87		-133	-60	0
	fluctuation [%]	3%	from average	-9%	5%	-29%	-7%	-7%	-17%	-4%	-23%	-5%		-8%	-4%	0%
Toravere (Estonia)	Yearly total [kWh/m^2]	997		964			1011	1011	864	968	969	964			1026	937
	fluctuation [kWh/m^2]	59	Deviation	-33			14	14	-133	-29	-28	-33			29	-60
	fluctuation [%]	6%	from average	-3%			1%	1%	-13%	-3%	-3%	-3%			3%	-6%
Vaulx-en-Velin (F)	Yearly total [kWh/m^2]	1316		1262	1348	1202	1252	1265	1119	1207		1221		1273	1308	1320
	fluctuation [kWh/m^2]	48	Deviation	-53	33	-114	-64	-51	-197	-108		-94		-42	-7	5
	fluctuation [%]	4%	from average	-4%	2%	-9%	-5%	-4%	-15%	-8%		-7%		-3%	-1%	0%
Wien (A)	Yearly total [kWh/m^2]	1215		1143	1181	1095	1105	1165	886	1108	1105	981		1093	1163	1183
	fluctuation [kWh/m^2]	69	Deviation	-72	-34	-120	-111	-50	-329	-107	-110	-235		-122	-52	-32
	fluctuation [%]	6%	from average	-6%	-3%	-10%	-9%	-4%	-27%	-9%	-9%	-19%		-10%	-4%	-3%
Zürich (CH)	Yearly total [kWh/m^2]	1134		1096	1198	1096	1231	1231	951	1112	1088	1094	1088	1106	1161	1200
	fluctuation [kWh/m^2]	85	Deviation	-38	64	-38	96	96	-184	-22	-46	-40	-46	-29	26	65
	fluctuation [%]	7%	from average	-3%	6%	-3%	8%	8%	-16%	-2%	-4%	-4%	-4%	-3%	2%	6%
Average	Yearly total [kWh/m^2]	1389		1300	1418	1308	1333	1343	1208	1310	1321	1307	1195	1270	1308	1365
all stations except	fluctuation [kWh/m^2]	50	Deviation	-60	37	-74	-27	-17	-152	-51	-59	-53	-70	-53	3	9
Davos & Sonnblick	fluctuation [%]	4%	from average	-5%	3%	-6%	-2%	-1%	-13%	-4%	-4%	-4%	-6%	-4%	0%	1%

Table III: Products comparison and annual variability for the European stations.
In the average column, the standard deviation calculated on the reference period is given in absolute and relative values.
The results for products situated within ± one standard deviation are given in blue.

available since the year 2004. For the six American sites, data for 10 to 14 years sequences are available, including satellite product derived by Suny. The comparison is done year by year as described on Figure 3 for the site of Geneva. The yearly total global irradiation is normalized to the 1999-2006 reference period average.

The results for the United States stations are illustrated with data from Table Mountain (CO) on Figure 7. The color codes are the same than on Figure 1.

From all the graphs given in the Annex (see http://www.cuepe.ch), the following conclusions can be drawn:

- even if the satellite derived data present some bias, the derived data interannual variation follows satisfactorily the ground measurements variation,
- the sites with potential snow cover (Davos, Sonnblick and Sion) show an important overestimation by Helioclim data, and an underestimation by SolarGis data,
- In Locarno, the year by year higher bias can be induced by the nearby mountains and lake,
- in Ilorin, the bias is probably due to a too low turbidity value used in the models. The turbidity measurements are not dense enough on the African continent.

For the American sites, the 1995 to 1998 period has to be considered separately, the deriving algorithm has changed in 1998. This can be seen on Figure 8 for the site of Table Mountain, where the 12 monthly averages are plotted separately for each year, derived data against ground measurements. Two linear best fits are also represented for the data before and after 1998. A higher dispersion and a different bias can clearly be seen on the figure for the beginning period.

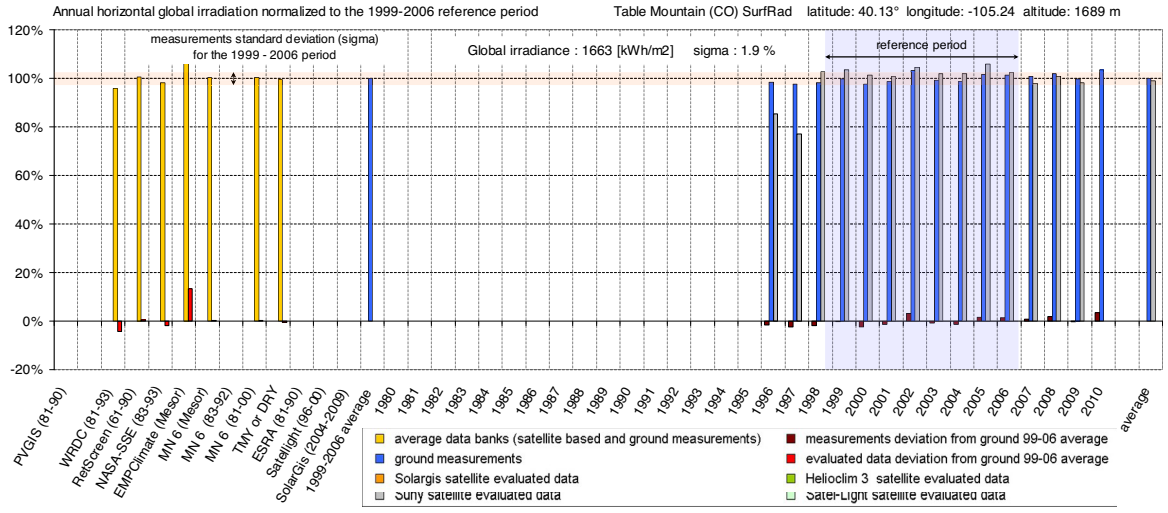

Figure 7: Relative total annual irradiation normalized to the average annual value over the reference period (1999-2006) for the site of Table Mountain (CO). The mean bias deviation is also given.

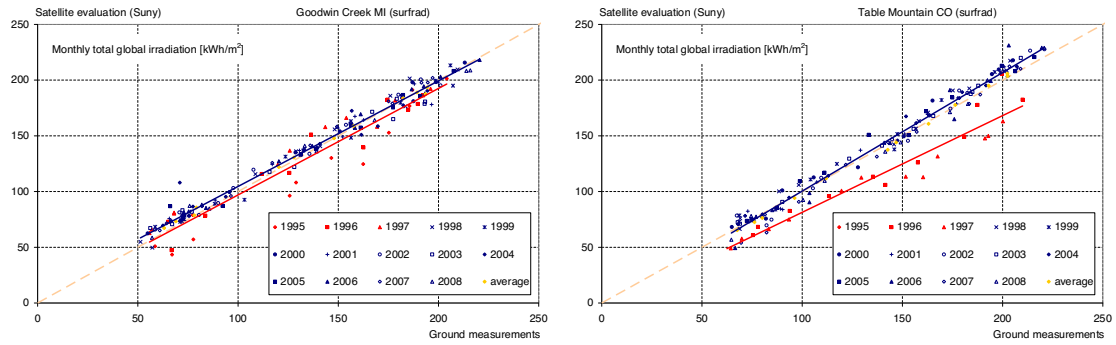

Figure 8: Derived monthly global irradiation versus the corresponding measurements, year by year for the station of Goodwin Creek and Table Mountain. A best fit is represented for two separate periods: before and after 1998.

In conclusion, except for some sites with specific ground or snow cover, an annual bias can be present,

depending on the site and the product. This could mainly be an aerosol optical depth and/or surface albedo effect. All the 4 tested products follow in a satisfactorily manner the year to year variability.

7. Conclusions

10 to 30 years of ground data acquired at 27 different sites are used to analyze the interannual variability of the solar irradiation and to compare it to average and/or interpolated data, software generated typical years and satellite derived data.

The main results are that the majority of the tested state of the art products give yearly values within the natural interannual variability of the solar irradiation. When dealing with specific year and «real» satellite derived data, their interannual variability follows in a satisfactorily manner the ground measurements, especially with the newest algorithms.

8. Acknowledgements

This comparative study could be performed thanks to the data provided by the MeteoSwiss (Swiss office of Meteorology and Climatology, http://www.meteoswiss.ch), FluxNet community (http://www.fluxdata.org) for the Spain sites, the BSRN network (http://www.gewex.org/bsrn.html) for Europe and part of Tamanrasset, the WRDC data set for Thessaloniki, Sonnblick, Wien and part of Tamanrasset (http://wrdc.mgo.rssi.ru), and the SurfRad network for the American sites (http://www.srrb.noaa.gov/surfrad).

9. References

Atwater M.A., Ball J.T. (1976) Comparison of radiation computations using observed and estimated precipitable water. Appl. Meteorol. 15, 1319-1320

Beyer H. G., Costanzo C., Heinemann D., (1996) Modifications of the Heliosat procedure for irradiance estimates from satellite data. Solar Energy, 56, pp 207-212.

Cano, D. et al. (1986): A Method for the Determination of Global Solar Radiation from Meteorological Satellite Data. Solar Energy 37, pp. 31-39

CIE (1994). Guide to Recommended Practice of Daylight Measurements. CIE 108, ISBN: 3 900 734 50x.

Derrien M., H. Gleau (2005) MSG/SEVIRI cloud mask and type from SAFNWC, International Journal of Remote Sensing, 26, 4707-4732.

ESRA (2000) The european solar radiation atlas. Coordinators : K. Scharmer, J. Greif,
ISBN : 2-911762-21-5

Ineichen P. and Perez R. (1999), Derivation of cloud index from geostationary satellites and application to the production of solar irradiance and daylight illuminance data. Th. and App. Clim., Vol. 64, N°1-2, pp. 119-130.

Ineichen P. (2008a) A broadband simplified version of the Solis clear sky model, Solar Energy 82, pp 758–762

Maxwell E. L. (1998): METSTAT – The solar radiation model used in the production of the National Solar Radiation Data Base (NSRDB) Solar Energy 62, 263-279

MeSor 2009. Management and exploitation of solar resource knowledge. Hoyer-Klick C. et al. Solar Paces 2009 Conference proceedings, Berlin, Germany, 2009.

Meteonorm 6.1, 2009. Global Meteorological Database for Engineers, Planners and Education, (http://www.meteotest.com)

Mishchenko M. et al., Aerosol retrievals over ocean using channel 1 and 2 AVHRR data. Appl. Opt., 38, 7325-7341, 1999

Mueller R.W, K.F. Dagestad, P. Ineichen et al. (2004) Rethinking satellite-based solar irradiance modelling: The SOLIS clear-sky module. Remote Sensing of Environment 91 (2004) 160–174

Perez R., P. Ineichen et al. (1992) Dynamic global to direct irradiance conversion models. ASHARE Trans. Res. Series, 1992, 354-369

Perez R., P. Ineichen et al. (2002): A New Operational Satellite-to-Irradiance Model. Solar Energy 73, 5, pp. 307-317

Perez R., P. Ineichen et al. (2003): Producing satellite-derived irradiances in complex arid terrain. Proc. ASES Annual Meeting, Austin, TX.

Randal D. L. et al. (1996): A new global water vapor dataset. Bulletin of the AMS (BAMS) - June, 1996 Vol. 77, No 6

Remund J. (2008), Updated Linke Turbidity and aerosol optical depth climatologies, IEA SHC Task 36 expert meeting, June 2008, Wels, Austria.

Rigollier C., Bauer O., Wald L. (2000) On the Clear Sky Model of the ESRA - European Solar Radiation Atlas - with Respect to the Heliosat Method. Solar Energy 68 (1), pp33-48.

Rigollier C., Lefèvre M, Wald L. (2004) The method heliosat-2 for deriving shortwave solar irradiance radiation from satellite imagesSolar Energy, 77(2), 159-169

Ruiz-Arias J.A. Et al., (2010). Spatial disaggregation of satellite-derived irradiance using a high resolution digital elevation model, accepted to Solar Energy.

Ruyter de Wildt M., G. Seiz, A. Gruen (2007) Operational snow mapping using multitemporal Meteosat SEVIRI imagery, Remote Sensing of Environment, 109, 29-41.

Schmetz J. (1989): Towards a Surface Radiation Climatology: Retrieval of Downward Irradiances from Satellites, Atmospheric Research, 23, 287-321

WMO (2008). Guide to meteorological instruments and methods of observation. See (http://www.wmo.int/)